Food Chemistry 371 (2022) 131095

Contents lists available at ScienceDirect

Food Chemistry

journal homepage: www.elsevier.com/locate/foodchem

The impact of gliadin and glutenin on the formation and structure of starch-lipid complexes

Xuemin Kang [a,b,c,1], Jie Sui [d,1], Xiaolei Zhang [a,b,c], Gao Wei [a,b,c], Bin Wang [a,b,c], Pengfei Liu [b,c], Lizhong Qiu [e], Hossny A. El-Banna [f], Bo Cui [a,b,c,*], A.M. Abd El-Aty [b,f,g,*]

[a] Department of Food Science and Engineering, Shandong Agricultural University, Taian 271018, China
[b] State Key Laboratory of Biobased Material and Green Papermaking, Qilu University of Technology, Shandong Academy of Sciences, Jinan 250353, China
[c] School of Food Science and Engineering, Qilu University of Technology, Shandong Academy of Sciences, Jinan, Shandong 250353, China
[d] Shandong Academy of Agricultural Science, Jinan, Shandong 250131, China
[e] Zhucheng Xingmao Corn Developing CO., LTD., Zhucheng, Shandong 262218, China
[f] Department of Pharmacology, Faculty of Veterinary Medicine, Cairo University, 12211 Giza, Egypt
[g] Department of Medical Pharmacology, Medical Faculty, Ataturk University, Erzurum, Turkey

ARTICLE INFO

Keywords:
WS-LA complexes
Gliadin
Glutenin
Physicochemical properties
in vitro digestion

ABSTRACT

This study evaluated the influence of the main gluten fractions (gliadin and glutenin) on the physicochemical properties of binary wheat starch-Lauric acid (WS-LA) complexes during heat processing to explore the complex structure and digestion of WS-LA in the presence of gluten. Ternary WS-LA-glutenin complexes were prepared at different pH (5.2 and 7), whereas WS-LA-gliadin was prepared using ethanol, and their physicochemical properties were analyzed. We found that the addition of glutenin displayed a sharper and higher diffraction peak than samples without protein, which increased short-range order structure (low full width at half-maximum (FWHM) of the band at 480 cm^{-1}) and good thermal stability (melting peak appeared at a higher temperature); the opposite was shown for gliadin. Even though glutenin increased the resistant starch (RS) content than WS-LA, all samples prepared in 65% ethanol showed higher RS content than WS-LA-glutenin samples. These findings might improve our understanding of the relationship between gliadin/glutenin and binary complexes and provide a theoretical basis for preparing starch-based foods with a low glycemic index.

1. Introduction

Starch, one of the essential ingredients in staple foods, contributes to approximately 60–70% of total energy consumed by the human body (Li et al., 2014). It is a mixture of two α-D-glucose polymers: lightly branched-amylose and highly branched-amylopectin that are hydrolyzed to glucose resulting in a rise in both insulin and blood sugar levels and insulin response (Cai & Shi, 2010). Hence, intake of starchy foods is limited for patients with chronic diseases, such as type 2 diabetes, (T2D) obesity, and cardiovascular diseases (Kang, Sui et al., 2021). Resistant starch (RS) that cannot be digested in the small intestine has attracted great interest in nutrition research and the food industry owing to its low blood glucose level and production of short-chain fatty acids (Zhang & Jin, 2011).

Presently, five types of RS have been described, produced by physical and chemical modification methods (Gutiérrez & Tovar, 2021). Starch-lipid complexes, or amylose–lipid complexes, are categorized as RS_5 (Sullivan, Hughes, & Small, 2018). Amylose forms a left-handed helix, which provides a place for hydrophobic ligands inside the helix. Then, ordered crystalline domains (which prevent contact with enzymes) are constructed with many helical structures and arranged together (Putseys, Lamberts & Delcour, 2010). Increasing the RS content in starch-rich foods has been proposed as a tool for managing obese patients with T2D because it can escape from enzymatic digestion. In turn, factors that would promote the formation of starch-lipid complexes have received considerable attention. For instance, experimental factors, such as amylose/amylopectin ratio, the amylose chain length and degree of saturation of C=C, the carbon chain length, and concentration of ligand,

* Corresponding authors at: Qilu University of Technology, Shandong Academy of Sciences, Daxue Road, Changqing District, Jinan, Shandong Province 250353, China.
E-mail address: abdelaty44@hotmail.com (A.M. Abd El-Aty).
[1] These authors contributed equally to this work.

https://doi.org/10.1016/j.foodchem.2021.131095
Received 17 May 2021; Received in revised form 6 September 2021; Accepted 6 September 2021
Available online 8 September 2021

which play a decisive role in the formation of the complex, have been extensively investigated over the past decades (Tufvesson, Wahlgren & Eliasson, 2003a; Tufvesson, Wahlgren & Eliasson, 2003b; Gelders, Vanderstukken, Goesaert & Delcour, 2004; Gelders, Goesaert & Delcour, 2005; Tang & Copeland, 2007; Zabar, Lesmes, Katz, Shimoni & Bianco-Peled, 2009; Putseys, Lamberts & Delcour, 2010). Further, external factors, including physical, chemical, enzymatic, and genetic methods, were all widely stated and reported; genetic modification improved the RS_2 in plants (Bhatnagar & Hanna, 1994; Le-Bail, Houinsou-Houssou, Kosta, Pontoire, Gore & Le-Bail, 2015; Schwall et al., 2000). During the last three years, researches carried out on RS_5 were all beyond starch-fatty acid complexes. Information on other starch-based complexes, such as starch-glycerol, starch-amino acids, starch-peptides, starch-proteins, starch-lipid-protein, starch-polyphenols, and starch-other polysaccharides (such as Chitosan), are all related to RS_5 (Zhang, Gladden, Guo, Tan & Kong, 2020; Liang et al., 2020; Lin, Yang, Chi & Ma, 2020; Zhang, Tian et al., 2020; Li, Li, Fox, Gidley & Dhital, 2021).

Starch and protein are thermodynamically incompatible to form complexes. However, hydrophobic or electrostatic interactions can affect their resistance to amylase digestion by increasing the ordered domain (Cai et al., 2020). Furthermore, the ternary complexes between starch-lipid-protein were illustrated by rapid visco analyzer (RVA) and high-performance size exclusion chromatography (HPSEC) (Zhang & Hamaker, 2003). The mechanism of ternary complexes of starch-monoglyceride-protein was reported by Chao et al. (2018). The interplay between starch, lipid, and proteins at different isoelectric points had been investigated by Lin et al. (2020). β-Lactoglobulin, whey protein isolate, and type-A gelatin, as model proteins, have been used to investigate the interplay between starch, lipid, or starch-lipid and proteins (Zheng et al., 2018). Nevertheless, and to the authors' knowledge, none of the studies focused on the effects of various proteins found in gluten on the formation of starch-lipid complexes. How proteins influenced the structure and digestibility of the starch-protein-lipid ternary system remained to be elucidated. Starch-rich foods (such as wheat, rice, and corn) are rich in protein, while their effect on functional or medicinal foods is still controversial.

Our previous work investigated the effect of gluten on the structure and digestive properties of prepared amylose–lipid complexes (Kang, Gao et al., 2021). Herein, the main components of gluten were purified to investigate their effects on the formation of complexes. A ternary system containing wheat starch (WS), lauric acid (LA), and gliadin or glutenin was used to assess the effects of gliadin and glutenin on the structure and physicochemical properties of binary or ternary complexes. Additionally, the *in vitro* digestibility of ternary starch-lipid-protein was also evaluated. The effects of the main gluten ingredients on starch-lipid digestibility were elucidated to provide ideas and models for processing food with slow digestion properties.

2. Materials and methods

2.1. Materials

Wheat starch (WS) was procured from Baby Suqian Biotechnology Co., Ltd. (Jiangsu, China). Gliadin was extracted from gluten secured from Enmiao Food Co., Ltd. (Henan, China). Lauric acid (LA) was purchased from Compass Biotechnology Co., Ltd. (Zhengzhou, China). Glutenin (CAS# 8002–80-0) was provided by Yuanye Biotechnology (Shanghai, China) with an N content of 13.42%. α-amylase of 100 U/mg (CAS# 9032–08-0) and amyloglucosidase of 10×10^4 U/mL (CAS# 9032–08-0) were obtained from Sigma-Aldrich (St. Louis, MO, USA) and Yuanye Biotechnology (Shanghai, China), respectively. All other chemicals were of analytical grade unless otherwise specified.

2.2. Extraction of gliadin from gluten

Gluten (30 g) and 1.5 L absolute alcohol (≥99.75%) were mixed with continuous stirring for 2 h at 30 °C. The suspension was withstanding for half an hour. Afterward, the supernatant (1 L) was mixed with 1 L distilled water, and gliadin precipitation occurred immediately. Further, the mixed solution was concentrated by Rotavapor (Shanghai Xiande Experimental Instrument Co., Ltd, Shanghai, China). After that, the residue was freeze-dried and passed through a 60 mesh sieve (Jiuding screen self-operated store, Hebei, China).

2.3. Preparation of ternary complexes

Preparation of WS-LA-glutenin sample: WS (6 g) was added to 100 g distilled water. Then, 0.18 g LA and/or 0.3 g glutenin was dispersed into WS suspension and heated at 90 °C for one hour with continuous stirring. After cooling to 30 °C, the mixture was washed with 50% ethanol and centrifuged (TDL-5-A, Shanghai Anting Scientific Instrument Co., Ltd., Shanghai, China) at 3000×*g* for 10 min. Finally, the residue was dried in an oven (Shanghai Boxun industrial Medical Instrument Factory, Shanghai, China) at 40 °C for 48 h and ground to pass through a 60-mesh sieve. Samples prepared by the above method were named "Water-WS-LA-glutenin". At the same time, an acetic acid buffer solution with pH 5.2 (away from the isoelectric point of glutenin 6.5 ~ 7.0) was used instead of distilled water to prepare "WS-LA-glutenin-pH 5.2" samples.

Preparation of WS-LA-gliadin sample: A 6 g WS was mixed with 100 g absolute alcohol and 50 mL distilled water. Then, 0.18 g LA and/or 0.3 g gliadin was dispersed in WS suspension and heated at 90 °C for one hour with continuous stirring. After cooling to 30 °C, the mixture was washed with absolute ethanol and centrifuged (TDL-5-A, Shanghai Anting Scientific Instrument Co., Ltd., Shanghai, China) at 3000 × *g* for 10 min. Finally, the residue was dried in an oven (Shanghai Boxun industrial Medical Instrument Factory, Shanghai, China) at 40 °C for 48 h and ground to a fine powder to pass through a 60-mesh sieve.

2.4. Fluorescence observation

WS-LA-glutenin (0.1 g), WS-LA-glutenin (pH 5.2), and WS-LA-gliadin powder were mixed with 0.5 mL (1% fluorescein isothiocyanate) and maintained at 90 °C for two hours with continuous stirring. Afterward, the samples were observed under the fluorescence polarizing microscope (Olympus, BX53-P, Tokyo, Japan).

2.5. X-ray diffraction (XRD)

The diffraction pattern of powder samples in section 2.3 was analyzed using X-ray diffraction analysis (Bruker AXS, Karlsruhe, Germany), executing at 40 kV, 40 mA, 2θ scanning from 5° to 40°.

2.6. Differential scanning calorimetry (DSC)

The powder sample (3 mg) was accurately weighed in an aluminum pan, to which 9 μL distilled water was added. Next, the sealed pans were placed at 20 °C for 12 h. Finally, the melting curves were determined at a temperature range of 20–140 °C using a NETZSCH DSC analyzer (DSC-200FC, Selb, Germany).

2.7. Atr-FTIR

The spectra of all samples were acquired by a NICOLET iS10 Thermo Fisher Scientific (Waltham, MA, USA). The infrared spectroscopy was recorded between 4000 cm^{-1} and 400 cm^{-1}.

2.8. LCM-Raman spectroscopy

The short-range molecular order of WS-LA samples with and without glutenin or gliadin was measured by a Renishaw Laser confocal Raman spectroscopy (Renishaw, Gloucestershire, UK) at a 785 nm green diode

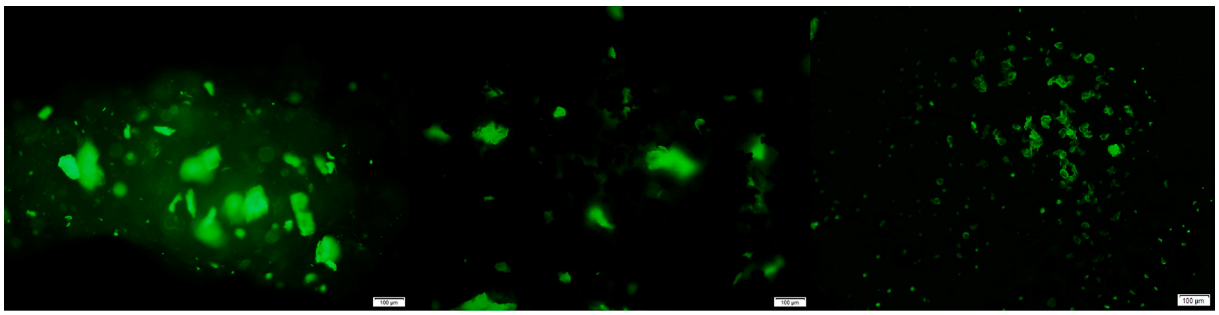

(a) (b) (c)

Fig. 1. Representative fluorescence microscopy images of WS-LA-glutenin and WS-LA-gliadin. (a): WS-LA-glutenin sample prepared in water; (b): WS-LA-glutenin sample prepared at pH 5.2; and (c): WS-LA-gliadin.

laser source. The spectra from 3200 to 100 cm^{-1} were obtained from at least five different positions per sample. The band's full width at half-maximum (FWHM) was measured at 480 cm^{-1} using the OriginPro8.5 (OriginLab, Northampton, MA, USA).

2.9. In vitro digestibility

In vitro hydrolysis of all samples was determined using the method described by Englyst & Cummings (1985) with minor modifications. Accurately weighted 40 mg powder sample was added to 35 mL acetate buffer (pH 5.2). Subsequently, a 10 mL mixed enzyme solution (290 U/mL α-amylase and 30 U/mL amyloglucosidases) was added to the

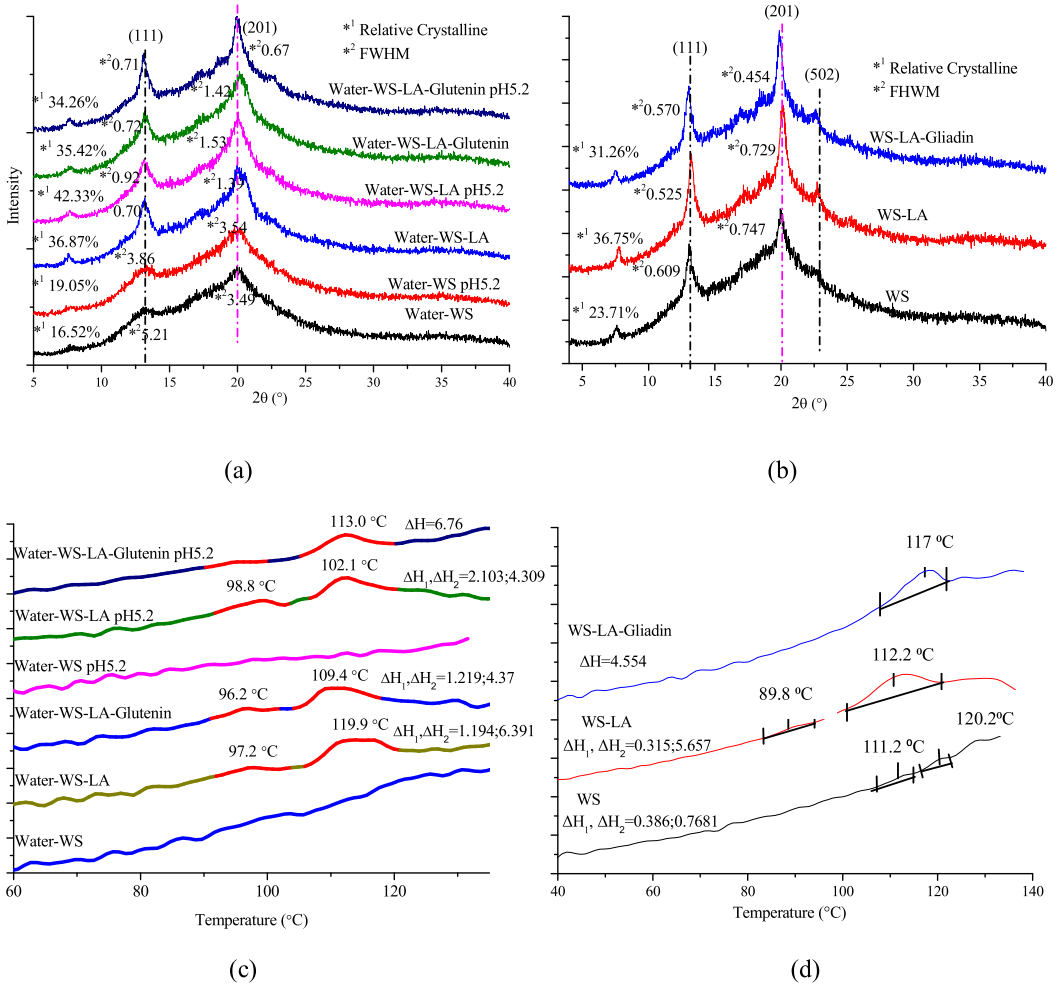

Fig. 2. X-ray diffraction (XRD) and DSC curves of WS, WS-LA, WS-LA-glutenin, and WS-LA-gliadin samples. (a) and (c): WS-LA-glutenin sample prepared in water and at pH 5.2; (b) and (d): WS-LA-gliadin.

mixture. Afterward, the suspension was placed in a water bath at 37 °C, with continuous stirring at 150 rpm for 4 h. The amount of glucose released during hydrolysis was determined at 20, 120, 180, and 240 min using an SBA-40D glucose analyzer (Shandong Academy of Sciences, Jinan, China).

2.10. Statistical analyses

The data are displayed as mean ± standard deviations (SDs). Significant differences between mean values were carried out using the software statistix 9. A $P < 0.05$ was assigned as statistically significant.

3. Results and discussion

Herein, we have tested whether ternary complexes WS-LA-gliadin/glutenin could be formed and whether the structures and properties of the complexes would be consistent with those of conventional binary complexes between starch and lipid. First, we compared the fluorescence distribution performance of WS-LA-gliadin/glutenin samples. Afterward, the diffraction pattern, DSC, ATR-FTIR, and LCM-Raman properties of WS-LA-gliadin/glutenin samples were compared with binary WS-LA complexes. Ultimately, the *in vitro* digestibility was investigated to gain insight regarding the digestion pattern of ternary samples.

3.1. Fluorescence microscope

The fluorescence distribution of WS-LA-gliadin/glutenin samples is shown in Fig. 1. The location of WS in ternary samples can be verified by fluorescence distribution (Ding et al., 2021). As shown in Fig. 1a & b, WS was wrapped around glutenin of WS-LA-glutenin (prepared in water, Fig. 1a), whereas the dispersed structure of WS-LA-glutenin prepared at pH 5.2 is presented in Fig. 1b. It is well-known that glutenin is soluble in dilute acid or alkali; therefore, evenly distributed; glutenin and WS could be seen in WS-LA-glutenin at a pH of 5.2. For the WS-LA-gliadin sample (Fig. 1c), the distribution of gliadin and WS became more uniform, resulting in shadows in the outer layer of almost every WS block structure. Furthermore, the distribution of glutenin and WS seems to be more dispersed than gliadin. The interplay between WS-LA-gliadin/glutenin will be further illustrated in the subsequent sections.

3.2. X-ray diffraction (XRD)

XRD patterns and relative crystallinity of WS-LA-gliadin/glutenin samples are shown in Fig. 2. As shown in Fig. 2 a & b, two prominent intensity peaks at $2\theta = 13.4713^\circ$ and 20.5207°, corresponding to (1 1 1) and (2 0 1) diffraction planes for the hexagonal structure at the same positions in a 2θ scale and one small peak around 2θ of 7.8400° were displayed, respectively (Cervantes-Ramírez et al. 2020). Prominent diffraction peaks at 13.7° and 20.3° are reflecting the formation of starch-lipid complexes with crystalline perfection. This finding denotes that the addition of gliadin and glutenin did not alter the crystalline type. Samples with protein did not show any other diffraction peaks related to the A or B crystalline structure (Zhang & Hamaker, 2003). According to Fig. 2a, the intensity of the diffraction peak was in the following order: water-WS < water-WS-LA-glutenin < water-WS-LA, whereas the intensity of all samples prepared in buffer solution (pH 5.2) was higher than the corresponding samples prepared in water (pH 7.0). This phenomenon illustrated that the pH and glutenin in the system influenced the crystalline structure of complexes. Compared with the water-WS sample, the diffraction peak became much sharper and higher following the addition of LA, forming WS-LA complexes. In addition, the intensity of the diffraction pattern of WS-LA-glutenin was weaker than the WS-LA sample without glutenin. Compared with WS-LA and WS-LA-glutenin samples prepared with water, the peak intensity of WS-LA-glutenin samples prepared at pH 5.2 was the strongest and the highest among all WS-LA and glutenin samples. This finding may be attributed to the fact that glutenin is likely to aggregate in water (pH ~ 7.0), inhibiting the interplay between WS and LA. With a pH solution far away from the isoelectric point, glutenin is fully extended. The hydrophobicity and hydrophilicity groups were fully exposed, creating a suitable environment for the interaction between starch and lipid to a certain extent. As shown in Fig. 2b, more substantial peaks were observed in the WS sample than in water-WS samples with pH 7.0 and 5.2. These results could be explained by the fact that ethanol, as a ligand, can also enter the helix cavity and form complexes with amylose (Gutiérrez & Tovar, 2021). Further, we found that the height and sharpness of the V-type crystalline diffraction peak of WS-LA-gliadin were weaker than the WS-LA sample in Fig. 2b. In other words, an ordered V-type crystalline structure was formed in WS-LA samples than those of WS-LA-gliadin samples. This behavior further elucidates that gliadin did not promote the interplay between WS and lipid. As gliadin is soluble in ethanol, it would adhere to the surface of WS granules during heating, thereby reducing the release of amylose.

The relative crystallinity (RC) of all samples is shown in Fig. 2. The value of RC was negatively correlated with the intensity of the diffraction peak. Compared with all WS-LA prepared in water (pH 7.0) and buffered solution with pH = 5.2 (Fig. 2a), samples prepared in ethanol (Fig. 2b) showed a higher and sharper diffraction peak, along with a lower RC value. Lower FWHM values of diffraction peak appeared at 13.7° and 20.4° around 0.57 and 0.45 were observed for WS-LA prepared in ethanol than WS-LA samples prepared in water and pH 5.2 solution. This finding could be ascribed to the fact that a more ordered and perfect V-type crystalline structure was formed in samples prepared in ethanol. Compared to WS-LA without protein, lower FWHM values were displayed in WS-LA samples with gliadin and glutenin, with less complex content. Therefore, combining the diffraction peak intensity and RC value results, we may infer that neither gliadin nor glutenin can promote starch-lipid complexes; however, their addition to the assay system can assist in forming ordered and perfect V-type crystalline structure.

3.3. Thermal properties

The DSC characteristic curves of all samples are shown in Fig. 2 (c & d). The characteristic peak measured over a temperature range of 20–140 °C is reflected by the thermal stability of binary and ternary complexes. It was reported that the thermal stability of starch was enhanced by the formation of starch-ligand complexes (Ding et al., 2019). That is to say, the appearance of melting peaks provides a shred of evidence for the existence of complexes (Ding et al., 2019; Falsafi et al., 2018). As can be seen in Fig. 2c, there was no melting peak for WS samples without LA. Double melting peaks were observed in WS-LA and WS-LA-glutenin samples (Fig. 2c), except for WS-LA-glutenin (pH 5.2). This finding was supported by a previous study stating that the crystalline structure of starch-lipid complexes can be divided into two distinct types: less ordered type I formed at low temperature, which results in a high nucleation rate coupled with randomly oriented individual helical segments (dissociated under melting point 105 °C); and type II complexes are obtained at a high reaction temperature, the nucleation rate is low, and melt above 105 °C (Putseys et al. 2010). However, only one melting peak was observed in the WS-LA-glutenin sample (pH 5.2), with T_p appeared at 113.3 °C. This finding designates that an ordered crystalline structure (type II) was formed in the sample incorporated with glutenin prepared under buffer solution with pH 5.2. A similar phenomenon was observed in Fig. 2d, where only one melting peak appeared in the WS-LA sample with gliadin. Therefore, we may conclude that adding glutenin or gliadin can promote the formation of ordered complexes.

ΔH values, which are used to reflect the content of complexes, are shown in Fig. 2. ΔH was increased with the addition of LA and decreased in the presence of glutenin or gliadin. Additionally, only ordered structure (type II) was displayed in samples with protein; however, the

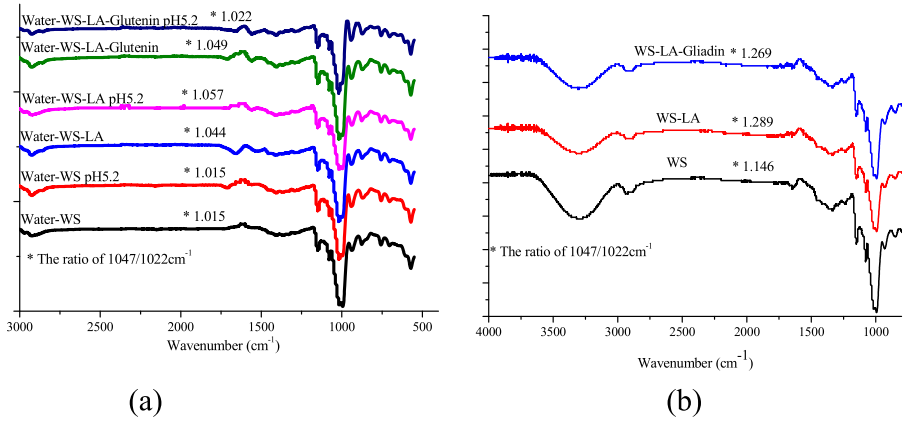

Fig. 3. ATR-FTIR spectra of WS, WS-LA, WS-LA-glutenin, and WS-LA-gliadin samples. (a): the ATR curves of WS-LA-glutenin sample prepared in water and at pH 5.2; (b): WS-LA-gliadin.

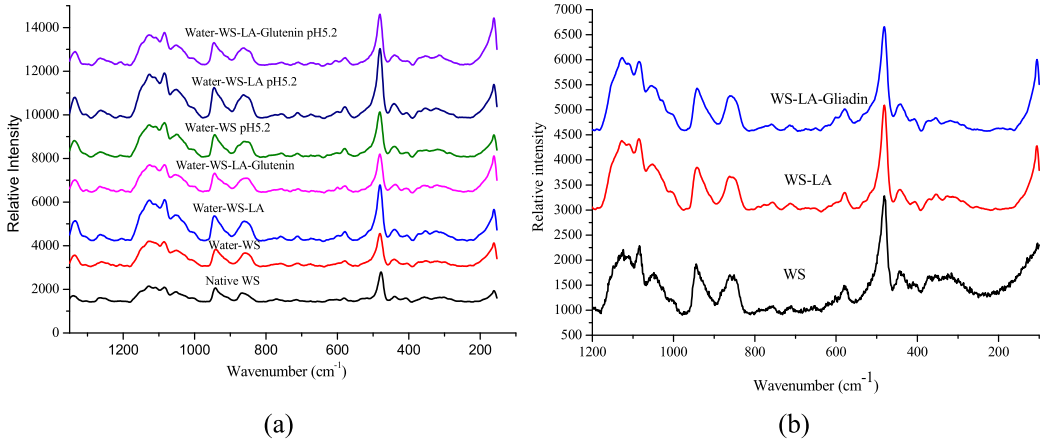

Fig. 4. LCM-Raman spectra of WS, WS-LA, WS-LA-glutenin, and WS-LA-gliadin samples. (a): WS-LA-glutenin sample prepared in water and at pH 5.2; (b): WS-LA-gliadin.

total ΔH was lower than samples without protein. Like XRD results (sharper and higher diffraction peaks with lower RC value), the total complex content was less, which is at variance with what has been reported by Zheng et al., 2018.

3.4. ATR-FTIR spectra

The FTIR spectra of WS, WS-LA, and WS-LA with and without proteins are shown in Fig. 3. In comparison with WS (Fig. 3a), two absorption bands were observed at 2850 and 1710 cm^{-1} in samples with LA, assigned to stretching vibration of C—H and carbonyl groups of LA, respectively (Eliasson & Krog, 1985). The band's intensity that appeared at 2850 cm^{-1} was decreased with glutenin and gliadin. This finding assumes that these two types of protein would attenuate the IR absorption of asymmetric C—H stretching vibration of LA. The carbonyl group of LA, which has absorption around 1705 cm^{-1}, disappeared in WS-LA samples with glutenin due to the encapsulation of glutenin. According to Fig. 3b, the disappearance of the absorption band at 2850 cm^{-1} may suggest the formation of WS-LA complexes. In addition, samples in Fig. 3a were prepared in ethanol, an excellent solvent to dissolve LA, resulting in no free fatty acid absorption at 2850 cm^{-1}. A weak absorption band at 1710 cm^{-1} (Fig. 3a) was at variance to what has been reported elsewhere, stating that the disappearance of the absorption band at 1710 cm^{-1} may indicate the formation of ternary complexes between starch, lipid, and protein (Zhang & Hamaker, 2003; Zheng et al., 2018). Moreover, the infrared spectra of 1047 cm^{-1} correspond to starch crystalline, whereas 1022 cm^{-1} represents the amorphous regions (Chi et al., 2017). The short-range order structure can be reflected by the ratio of 1047/1022 cm^{-1}; with the addition of LA, gliadin, and glutenin, the ratio increases, which means a more ordered structure was formed. As shown in Fig. 3 (a & b), a higher absorbance ratio at 1047/1022 cm^{-1} was seen in pH 5.2- and ethanol-WS-LA samples than that with proteins, the finding which is consistent with the results of XRD.

Table 1
The full width at half-maximum (FWHM) of Raman band at 480 cm^{-1} for all samples.

Samples	FWHM at 480 cm^{-1}		
	Water (pH 7.0)	pH 5.2	Ethanol
WS	$20.06729^{a} \pm 0.58258$	$20.29897^{a} \pm 0.72361$	$23.54096^{a} \pm 0.97506$
WS-LA	$19.98117^{a} \pm 0.71974$	$18.34128^{b} \pm 0.68040$	$17.97051^{c} \pm 0.68590$
WS-LA-glutenin/ gliadin	$19.56378^{a} \pm 0.69955$	$19.36614^{ab} \pm 0.65819$	$18.69999^{b} \pm 0.69373$

a-c: Different letters within the same column indicate significant differences ($P < 0.05$).

3.5. LCM-Raman spectroscopy

LCM-Raman can determine the short-range ordered structure of WS,

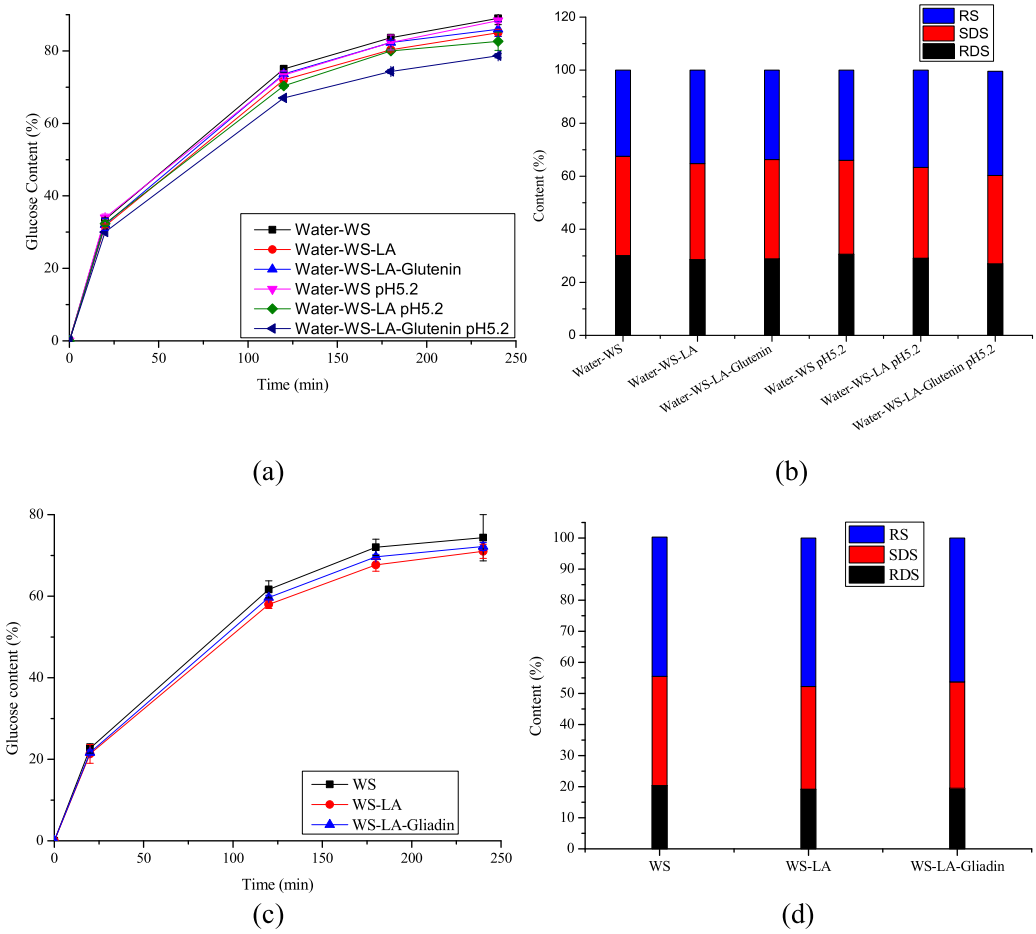

Fig. 5. In vitro digestion of WS, WS-LA, WS-LA-glutenin, and WS-LA-gliadin samples. (a) and (c): the glucose content of WS-LA-glutenin sample prepared in water and at pH 5.2 and WS-LA-gliadin, respectively. (b) and (d): contents of rapidly digestible starch (RDS), slowly digestible starch (SDS), and resistant starch (RS).

WS-LA, and WS-LA with glutenin or gliadin. Based on the previous studies, the full width at half-maximum (FWHM) of the band at 480 cm^{-1} was susceptible to changes in the short-range molecular order of starch, and a smaller FWHM value means a higher degree of structural order (Zheng et al., 2018; Wang, Zhang, Wang & Copeland, 2016). The Raman spectroscopy and the FWHM value are shown in Fig. 4 and Table 1, respectively. There were no significant differences ($P > 0.05$) for FWHM values in WS, WS-LA, and WS-LA-glutenin samples prepared in water (pH 7.0). This finding indicates the presence of complexes with short-range disordered molecular. Significant differences ($P < 0.05$) were found in WS, WS-LA, and WS-LA-glutenin samples under pH 5.2. Little difference was observed for WS-LA-glutenin, indicating less ordered short-range molecular complexes were formed with the addition of glutenin. In addition, there were significant differences ($P < 0.05$) between WS, WS-LA, and WS-LA-gliadin samples prepared in ethanol ($P < 0.05$). This finding suggests the formation of complexes with a higher degree of ordered structure in WS-LA and WS-LA-gliadin samples. It has to be noted that the FWHM value of the WS-LA sample with gliadin was lower than the sample without gliadin addition. These observations further indicate that LA structure impacts the short-range ordered structures of WS-LA complexes higher than glutenin and gliadin on WS-LA-protein complexes. The FWHM values of all WS-LA-protein systems were higher than those of the respective WS-LA systems, indicating that the binary WS-LA complexes without protein have a greater degree of short-range molecular order. This finding is at variance with Zheng et al. (2018) study.

3.6. *In vitro digestibility*

The *in vitro* enzyme digestion of WS, WS-LA, and WS-LA with protein is shown in Fig. 5. All samples showed similar digestion trends: a rapid increase followed by a plateau after 120 min. According to Fig. 5a, the highest glucose content was observed in water-WS and water-WS-pH 5.2 during the process of *in vitro* digestion. After interaction with LA and glutenin, the glucose content significantly decreased ($P < 0.05$), especially for WS-LA-glutenin (pH 5.2). As shown in Fig. 5b, RS (35.2%) content was dramatically increased with the addition of LA to the water-WA-LA sample, and the values of SDS (37.4031%) and RS (33.6997%) content were remained unchanged in water-WS-LA-glutenin. Further, glutenin increased the RS content (39.3%) and reduced SDS (33.3%) and RDS (27%) in the WS-LA-glutenin sample (pH 5.2). Glutenin retard the contact between starch and enzyme, thereby slowing down starch digestion. This result illustrates that both pH and glutenin are the factors that would affect the digestibility of WS-LA samples. That is to say, the composition of protein and the pH (the isoelectric point of protein) of raw materials are the critical factors in determining the digestibility of starchy food.

According to Fig. 5 c & d, WS displayed low glucose content than WS samples in Fig. 5 a &b. This finding could be ascribed to the formation of WS-alcohol complexes during the heating process of the WS sample. This result is in line with the XRD analysis: typical V-type diffraction peaks were observed that were related to the digestion of starch. Furthermore, lower glucose content was revealed in WS-LA and WS-LA-gliadin samples than corresponding samples in Fig. 5 a & b. It was in line with DSC's peak temperature (Tp): the higher T_p value means a perfect crystalline

structure in samples, reflected by slower digestion. In addition, the RS content was reduced from 47.80 to 46.3%, and SDS was increased from 33% to 34.2% with adding gliadin compared with the WS-LA sample. Perfect and ordered complexes were formed with the addition of proteins. At the same time, its content was limited, which was reflected by XRD and DSC that sharper diffraction peaks with lower RC value and significant type II with lower ΔH was observed. Additionally, ternary complexes between WS, LA, and glutenin showed higher resistance to enzymatic digestion than WS-LA-gliadin. In sum, protein types would significantly affect the formation of ordered structures and influence the digestibility of the starch-lipids-protein complexes.

4. Conclusion

The impacts of protein (gliadin and glutenin) on the structures and digestibility of WS-LA complexes were investigated. A fluorescence microscope demonstrated the distribution of gliadin and glutenin in the ternary sample. Further, the analysis of XRD and DSC suggested the formation of a perfect crystalline structure (type II) with the addition of protein, implying that gliadin and glutenin would promote the ordered WS-LA structure. Further, pH is considered one of the principal factors that would affect the structure of WS-LA complexes. On the one hand, the addition of protein decreased WS-LA short-range ordered structures, which increased the digestibility. Further, protein could cover the surface of WS granules, thereby reducing the contact between WS and LA. These results might have practical significance for SDS and RS-based food preparation and the management of chronic diseases, such as T2D and cardiovascular diseases.

Declaration of Competing Interest

The authors declare that they have no known competing financial interests or personal relationships that could have appeared to influence the work reported in this paper.

Acknowledgments

The financial supports received from the National Key Research & Development Program in China (2019YFD1002704), the Key Research and Development Program of Shandong Province (2017YYSP024), Special Funds for Taishan Scholars Project, the Innovation Team of Jinan City (2018GXRC004), Shandong major projects of independent innovation (2019JZZY010722), The Science and Technology Demonstration Project of "Bohai Granary" of Shandong Province (2019BHLC002), and Major agricultural application technology innovation projects of Shandong Province (SF1405303301), Innovation Pilot Project of Integration of Science, Education and Industry of Shandong Province (2020KJC-ZD011) are acknowledged.

References

Bhatnagar, S., & Hanna, M. A. (1994). Extrusion processing conditions for amylose-lipid complexing. *Cereal Chemistry, 71*, 587–593.

Cai, J. J., Chao, C., Niu, B., Copeland, L., Wang, S., & Wang, S. J. (2020). New insight into the interactions among starch, lipid and protein in model systems with different starches. *Food Hydrocolloids, 112*, Article 106323.

Cai, L., & Shi, Y.-C. (2010). Structure and digestibility of crystalline short-chain amylose from debranched waxy wheat, waxy maize, and waxy potato starches. *Carbohydrate Polymers, 79*(4), 1117–1123.

Cervantes-Ramírez, J. E., Cabrera-Ramirez, A. H., Morales-Sánchez, E., Rodriguez-García, M. E., Reyes-Vega, M.d.l. L., Ramírez-Jiménez, A. K., et al. (2020). Amylose-lipid complex formation from extruded maize starch mixed with fatty acids. *Carbohydrate Polymers, 246*, 116555. https://doi.org/10.1016/j.carbpol.2020.116555.

Chao, C., Cai, J., Yu, J., Copeland, L., Wang, S., & Wang, S. (2018). Toward a better understanding of starch-monoglyceride-protein interactions. *Journal of Agricultural and Food Chemistry, 66*(50), 13253–13259.

Chi, C., Li, X., Zhang, Y., Chen, L., Li, L., & Wang, Z. (2017). Digestibility and supramolecular structural changes of maize starch by non-covalent interactions with gallic acid. *Food & function, 8*(2), 720–730.

Ding, L.i., Huang, Q., Li, H., Wang, Z., Fu, X., & Zhang, B. (2019). Controlled gelatinization of potato parenchyma cells under excess water condition: Structural and *in vitro* digestion properties of starch. *Food & Function, 10*(9), 5312–5322.

Ding, Y. Y., Cheng, J. J., Lin, Q. Y., Wang, Q. Y., Wang, J. R., & Yu, G. P. (2021). Effects of endogenous proteins and lipids on structural, thermal, rheological, and pasting properties and digestibility of adlay seed (*coix lacryma-jobi* L.) starch-sciencedirect. *Food Hydrocolloids, 111*, Article 103254.

Eliasson, A.-C., & Krog, N. (1985). Physical properties of amylosemonoglyceride complexes. *Journal of Cereal Science, 3*(3), 239–248.

Englyst, H. N., & Cummings, J. H. (1985). Digestion of the polysaccharides of some cereal foods in the human small intestine. *American Journal of Clinical Nutrition, 42*(5), 778.

Falsafi, S. R., Maghsoudlou, Y., Rostamabadi, H., Rostamabadi, M. M., Hamedi, H., & Hosseini, S. M. H. (2018). Preparation of physically modified oat starch with different sonication treatments. *Food Hydrocolloids, 89*, 311–320.

Gelders, G. G., Goesaert, H., & Delcour, J. A. (2005). Potato phosphorylase catalyzed synthesis of amylose-lipid complexes. *Biomacromolecules, 6*(5), 2622–2629.

Gelders, G. G., Vanderstukken, T. C., Goesaert, H., & Delcour, J. A. (2004). Amyloseelipid complexation: A new fractionation method. *Carbohydrate Polymers, 56*, 447–458.

Gutiérrez, T. J., & Tovar, J. (2021). Update of the concept of type 5 resistant starch (RS5): Self-assembled starch V-type complexes. *Trends in Food Science & Technology, 109*, 711–724.

Kang, X., Sui, J., Qiu, H., Sun, C., Zhang, H., Cui, B.o., et al. (2021). Effects of wheat protein on the formation and structural properties of starch-lipid complexes in real noodles incorporated with fatty acids of varying chain lengths. *LWT-Food Science and Technology, 144*, 111271. https://doi.org/10.1016/j.lwt.2021.111271.

Kang, X., Gao, W., Wang, B., Yu, B., Zhang, H., Cui, B.o., et al. (2021). Effects of proteins on the structure, physicochemical properties, and *in vitro* digestibility of wheat starch-lauric acid complexes under various cooking methods. *International Journal of Biological Macromolecules, 182*, 1112–1119.

Le-Bail, P., Houinsou-Houssou, B., Kosta, M., Pontoire, B., Gore, E., & Le-Bail, A. (2015). Molecular encapsulation of linoleic and linolenic acids by amylose using hydrothermal and high-pressure treatments. *Food Research International, 67*, 223–229.

Li, H.-T., Li, Z., Fox, G. P., Gidley, M. J., & Dhital, S. (2021). Protein-starch matrix plays a key role in enzymic digestion of high-amylose wheat noodle. *Food Chemistry, 336*, 127719. https://doi.org/10.1016/j.foodchem.2020.127719.

Li, X., Miao, M., Jiang, H., Xue, J., Jiang, B.o., Zhang, T., et al. (2014). Partial branching enzyme treatment increases the low glycaemic property and α-1,6 branching ratio of maize starch. *Food Chemistry, 164*, 502–509.

Liang, Z., Chen, X.u., Luo, J., Zhao, H.-B., Yang, Z., & Zhu, J. (2020). Addition of amino acids to modulate structural, physicochemical, and digestive properties of corn starch-amino acid complexes under hydrothermal treatment. *International Journal of Biological Macromolecules, 160*, 741–749.

Lin, L.i., Yang, H., Chi, C., & Ma, X. (2020). Effect of protein types on structure and digestibility of starch-protein-lipids complexes. *LWT-Food Science and Technology, 134*, 110175. https://doi.org/10.1016/j.lwt.2020.110175.

Putseys, J. A., Lamberts, L., & Delcour, J. A. (2010). Amylose inclusion complexes: Formation, identity and physico-chemical properties. *Journal of Cereal Science, 51*(3), 238–247.

Schwall, G. P., Safford, R., Westcott, R. J., Jeffcoat, R., Tayal, A., Shi, Y.-C., et al. (2000). Production of very-high-amylose potato starch by inhibition of SBE a and b. *Nature Biotechnology, 18*(5), 551–554.

Sullivan, W. R., Hughes, J. G., Cockman, R. W., & Small, D. M. (2018). The effects of temperature on the crystalline properties and resistant starch during storage of white bread. *Food Chemistry, 228*, 57–61.

Tang, M., & Copeland, L. (2007). Analysis of complexes between lipids and wheat starch. *Carbohydrate Polymers, 67*(1), 80–85.

Tufvesson, F., Wahlgren, M., & Eliasson, A. C. (2003). Formation of amyloseelipid complexes and effects of temperature treatment. part 2. Fatty acids. *Starch-Stärke, 55*, 138–149.

Tufvesson, F., Wahlgren, M., & Eliasson, A.-C. (2003). Formation of amylose-lipid complexes and effects of temperature treatment. Part 1. Monoglycerides. *Starch-Stärke, 55*(2), 61–71.

Wang, S., Zhang, X., Wang, S., & Copeland, L. (2016). Changes of multiscale structure during mimicked DSC heating reveal the nature of starch gelatinization. *Scientific Reports, 6*, 28271.

Zabar, S., Lesmes, U., Katz, I., Shimoni, E., & Bianco-Peled, H. (2009). Studying different dimensions of amylose-long chain fatty acid complexes: Molecular, nano and micro level characteristics. *Food Hydrocolloids, 23*(7), 1918–1925.

Zhang, G., & Hamaker, B. R. (2003). A three component interaction among starch, protein, and free fatty acids revealed by pasting profiles. *Journal of Agricultural and Food Chemistry, 51*(9), 2797–2800.

Zhang, H., & Jin, Z. (2011). Preparation of resistant starch by hydrolysis of maize starch with pullulanase. *Carbohydrate Polymers, 83*(2), 865–867.

Zhang, Y., Gladden, I., Guo, J., Tan, L., & Kong, L. (2020). Enzymatic digestion of amylose and high amylose maize starch inclusion complexes with alkyl gallates. *Food Hydrocolloids, 108*, 106009. https://doi.org/10.1016/j.foodhyd.2020.106009.

Zhang, Z., Tian, J., Fang, H., Zhang, H., Kong, X., Wu, D., et al. (2020). Physicochemical and digestion properties of potato starch were modified by complexing with grape seed proanthocyanidins. *Molecules, 25*(5), 1123. https://doi.org/10.3390/molecules25051123.

Zheng, M., Chao, C., Yu, J., Copeland, L., Wang, S., & Wang, S. (2018). Effects of chain length and degree of unsaturation of fatty acids on structure and *in vitro* digestibility of starch-protein-fatty acid complexes. *Journal of Agricultural and Food Chemistry, 66*(8), 1872–1880.